Xerographic Transfer and Charging by Means of the Piezoelectric Effect*

Joseph M. Crowley†

Electrostatic Applications, 16525 Jackson Oaks Drive, Morgan Hill, California 95037

Christopher Snelling† **and Dale Mashtare**†

Xerox EXITE Laboratory, 317 Main Street, East Rochester, New York

Bending a ferroelectric polymer produces internal polarization that can lead to external electric fields. Both theoretical and experimental analyses have been carried out to predict the magnitudes of these fields, using flexible ferroelectric polymer materials based on polyvinylidenefluoride. The output depends on the thickness of the film, the bending radius, and a measured piezoelectric coefficient that is characteristic of the material. The electric field can exceed the levels now used in xerographic transfer and charging subsystems, suggesting that piezoelectric bending could replace conventional high-voltage power supplies and corona devices. Examples of applications to copier and printer subsystems are described.

Journal of Imaging Science and Technology 40: 285–290 (1996)

Introduction

Many of the subsystems in copiers and laser printers require sources of high electric fields, generally at low current levels. In conventional machines, this need is usually met by incorporating high-voltage power supplies feeding the coronas and bias rolls that perform such processes as precharge and transfer. The need for these components limits portability and energy conservation, in addition to adding cost and weight. Fortunately, there is a simpler solution that promises to eliminate these penalties. This method, based on the piezoelectric properties of electrically poled polyvinylidenefluoride (PVDF) films, is described in this report.

Ferroelectric films have been used for many applications, such as microphones and pressure sensors,[1] where they typically convert bending strain into voltage, which is recovered from electrodes attached to both sides of the film. These devices are commonly characterized as bimorphs or unimorphs, depending on the number and orientation of polymer layers between the two electrodes.

The devices described here differ from conventional ferroelectric devices in that only one surface of the film has an attached electrode. The other surface is left exposed to the air. This allows the electric field generated by the bending to extend from the film. We call this configuration a *xeromorph* to indicate its suitability for xerographic applications and to distinguish it from earlier applications that were concerned with generating voltages, rather than fields.

In this report, we discuss the relation between the electric field generation and the piezoelectric properties of the film and present the results of experiments designed to measure the relevant piezoelectric coefficient. Formulas for the magnitude of the external fields are then derived and applied to two useful configurations called the *unimorph* and the *bimorph*. These configurations are then applied to typical xerographic subsystems.

Voltage and Field Generation

When a piezoelectric sheet is bent, it develops an internal electric field that is proportional to the deformation.[2] The electric field satisfies an equation of the form

$$D = \varepsilon E + P. \tag{1}$$

The polarization field P is a function of position, because it depends on the local strain S.

$$P = P(z) = \varepsilon\beta S(z). \tag{2}$$

Here we assume that the strain is given, so that the stress–strain relation for the material is not needed. Unlike ordinary dielectrics, its polarization cannot be represented by a simple relation between the applied field and its polarizability. Instead, it acts more like a variable charge source distributed throughout the thickness of the film. The coefficient β is a piezoelectric constant of the material, which can be calculated from other material properties or measured directly.

To illustrate the basic operation of the device, we assume that both the bulk and the surface of the film are uncharged and that there is no external field. The only source of electrostatic fields is the polarization that appears in the material when it is bent. With no free charge, and no external fields, the E field in the layer is given from Eq. 1 as

$$E(z) = -\frac{P(z)}{\varepsilon}. \tag{3}$$

The E field inside the layer cannot be uniform, because it changes with P, which in turn depends on the local strain. The surface potential at the top of the layer can be obtained by integrating the E field across the piezoelectric

Original manuscript received February 2, 1996. Revised May 6, 1996.

* Presented in part at IS&T's 11th International Congress on Advances in Non-Impact Printing Technologies, October 29–November 3, 1995. Hilton Head, SC.

† IS&T Member

layer from the ground at $z = 0$ up to the free surface at $z = b$, to give the surface potential of the piezoelectric layer as

$$V_p = -\int_0^b E(z)dz = \int_0^b \frac{P(z)}{\varepsilon}dz \tag{4}$$

or, in terms of the piezoelectric coefficient β and the strain,

$$V_p = \beta\int_0^b S(z)dz. \tag{5}$$

Thus we need to determine the strain distribution in a particular configuration before we can calculate the open circuit voltage.

Bimorph Generators

When a uniform sheet is bent, it compresses on the inside of the bend and expands on the outside. Even if the sheet is piezoelectric, the voltages across each half of the layer cancel each other, giving zero potential difference across the entire sheet. To circumvent this problem, we fabricated more complicated arrangements of piezoelectric films. One of these is a bimorph, in which two electrically poled PVDF sheets (Kynar brand, supplied by AMP) were laminated together with their poling directions opposed, as shown in Fig. 1. Typically, the structure comprises two 4-mil (0.1-mm) Kynar sheets bonded by an adhesive, giving a total thickness of 0.22 mm. When this laminated sheet is bent, the neutral plane is at $z = 0$ in the figure. Above this plane, the positive strain in the outside layer generates a positive voltage. The negative strain in the inner layer also generates a positive voltage, due to the reversal of the poling direction in the bimorph. The net effect generates twice the voltage obtained for a single sheet.

The surface potential arising in this arrangement is therefore

$$V_p = 2\int_0^{b/2} \beta S dz\,. \tag{6}$$

The strain is given by

$$S = \frac{z}{R}, \tag{7}$$

so the voltage integral gives the open circuit piezoelectric voltage of the bimorph as

$$V_p = \frac{\beta b^2}{4R}. \tag{8}$$

These equations can be compared to the experimental results obtained with handmade bimorphs. The laminate was then bent around circular forms of different diameters, and the surface potential measured with an electrostatic voltmeter. The measurements obtained in these tests are shown in Fig. 2.

Both the thickness and the curvature are known from the geometry of the experiment, so once the piezoelectric coefficient β is known, the open circuit voltage predicted by the model can be calculated. The data sheets for the material used in these experiments (Kynar) did not give this coefficient directly, but they did give ranges of values for the d coefficient, dielectric constant, and Young's modulus. The β coefficient can be obtained from these parameters by using standard piezoelectric tensor relations.[3] Using the largest range given in the Kynar data sheets allows us to conclude that the β coefficient is in the range

$$261\text{V}/\mu\text{m} < \beta < 770\text{V}/\mu\text{m}. \tag{9}$$

Surface potential predictions based on these limits are also shown in Fig. 2 as a function of the curvature. The experimental measurements of surface potential are bracketed by the model predictions, indicating that the magnitude of the potential can be estimated from the basic properties of the material. An apparent value of the piezoelectric coefficient β was determined by fitting the data points to Eq. 8. This curve passes very close to each of the data points, which further indicates that the voltage has the predicted dependence on the radius of curvature. The fitted value, which will be used in the remainder of this report, is

$$\beta = 431\text{V}/\mu\text{m}. \tag{10}$$

Although the surface potential is easy to measure and serves as an indication of the magnitude of the effect, it is not the most useful quantity for application design. In most xerographic subsystems, it is the electric field and not the surface potential that controls the process. This E field

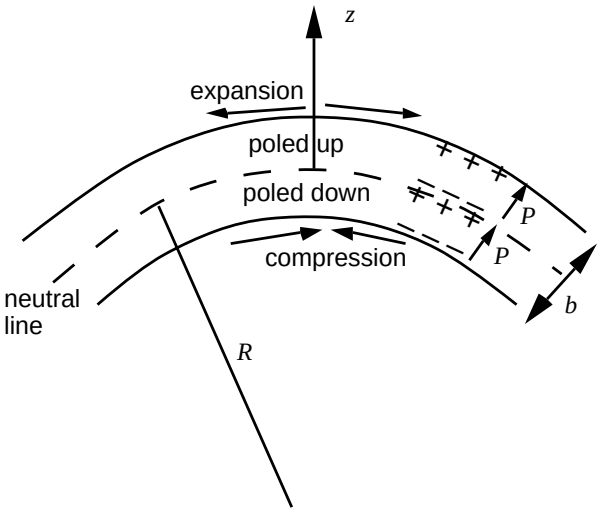

Figure 1. Bent bimorph film.

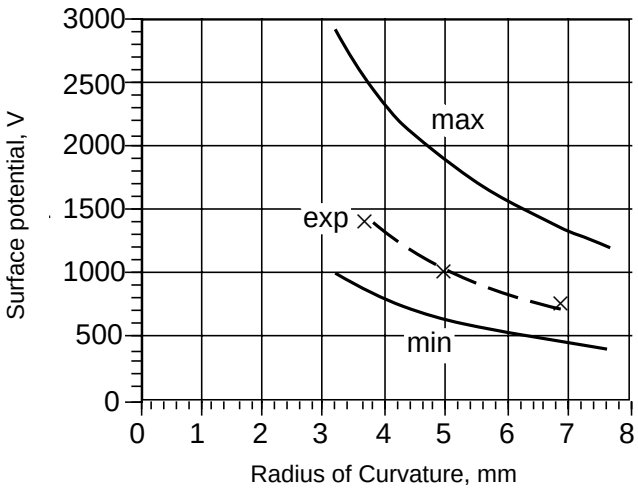

Figure 2. Surface potential of a bent Kynar bimorph.

can be calculated from the basic electrostatic relations for the geometry involved.

A typical geometry involves a piezoelectric layer with a grounded electrode attached to one side and an air gap of finite thickness a on the other, as shown in Fig. 3. As before, both the surface charge and the bulk charge are assumed to be zero. This condition need not be true in practice, because insulating surfaces often become charged triboelectrically. In addition, the fields generated by piezoelectric effects can attract ions from the surrounding atmosphere. In the applications described here, however, this surface charging was reduced to negligible levels by standard xerographic techniques. For these applications, therefore, the assumption is valid, and the D vectors are therefore uniform in both layers and equal to each other,

$$D = \varepsilon_0 E_a = \varepsilon E_b + P. \tag{11}$$

In this case, however, the E field does not vanish outside the xeromorph. In fact, it is the external E field that does the useful work in the xerographic system. Because there are grounded electrodes above the air layer and below the piezoelectric layer, the net voltage drop across both layers must vanish,

$$aE_a + \int_0^b E_b dz = 0 \tag{12}$$

Solving these equations gives the field in the air as

$$E_a = \frac{V_p}{a + b/\kappa} = \beta\kappa \frac{b}{4R} \frac{b/\kappa}{(a + b/\kappa)}. \tag{13}$$

From this expression, it is clear that the electric field will be largest when the air gap a is small compared with the dielectric thickness of the piezoelectric layer, $a << b/\kappa$. In this limit the E field in the air reaches a maximum value of

$$E_{a,\max} = \frac{\beta\kappa}{2} \frac{b}{2R}. \tag{14}$$

Note that it does not increase indefinitely as the air gap a becomes smaller, but reaches a finite value.

The second term $b/2R$ in Eq. 15 is the elastic strain at the surface, which should be limited to a value well below the elastic limit of the piezoelectric layer. Denoting the maximum strain that we are willing to tolerate in a given application by $S_{\max}$, we can then determine the largest electric field that can be generated in a small air gap. This field is

$$E_{a,\max} = \frac{1}{2}\beta\kappa S_{\max}. \tag{15}$$

For a typical dielectric constant for Kynar ($\kappa = 12$) and a conservative limit of 1% strain, the E field in the air could become as large as

$$E_{a,\max} = 51.7 \text{ V}/\mu\text{m}, \tag{16}$$

which is slightly smaller than the breakdown of air in a very small gap (68 V/μm) and much larger than the breakdown field of a wide gap (3 V/μm). Thus a small gap next to a bent piezoelectric film would experience electric fields almost as large as any in current xerographic engines, even with a 1% strain. This is a very encouraging result, because it indicates that currently available materials can generate enough field to replace most conventional high-voltage supplies in subsystems like transfer and charging.

Unimorph Generators

The maximum output can be obtained with any bimorph of a given thickness if the roller radius is chosen appropriately. In many cases, however, the roller radius is constrained by practical design. If it is too large, then the output will be reduced below its maximum value, so larger rollers may not work well with bimorphs. In this situation, an alternative fabrication offers an easier way to obtain the desired output. Instead of laminating two films back to back, a single piezoelectric film can be laminated to a thicker substrate that has no piezoelectric properties. This substrate could be any type of material that can be bent, including metals and plastics. When this combination is bent, the piezoelectric film at the surface of the thick substrate is stretched much more than it would be in a bimorph, so it generates a larger output.

An example of such a belt is shown in Fig. 4. The total thickness of the belt is again given by b. The thickness of the active piezoelectric layer on the outside of the bend is given by h. This layer is open to the air above it and is grounded at the point where it is laminated to the substrate. In this figure, the active layer is only in the upper half of the belt, so it experiences only stretching deformation. The open circuit voltage developed by this arrangement is given by the same formula as for the bimorph, but the integral is

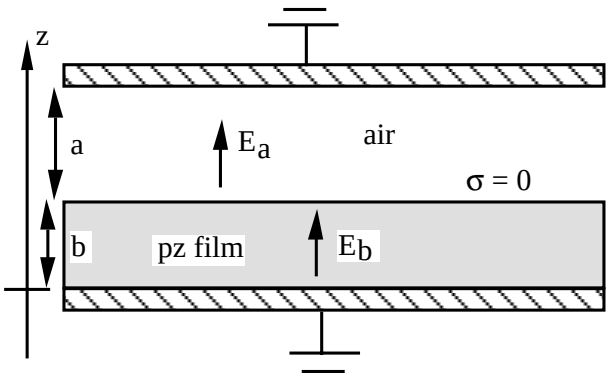

Figure 3. Air gap above a piezoelectric voltage generator.

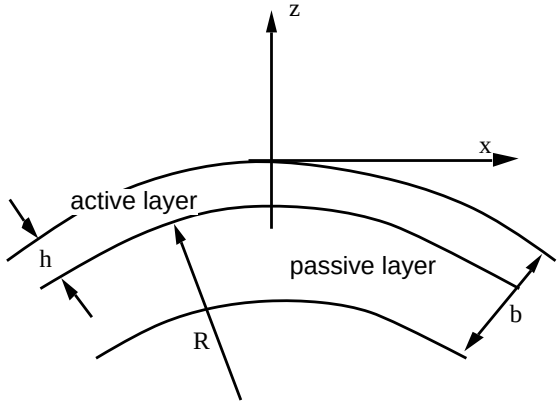

Figure 4. Unimorph geometry.

evaluated only over the active region and not over the entire belt,

$$V_p = \int_{b/2-h}^{b/2} \frac{\beta z}{R} dz = \frac{\beta h(b-h)}{2R}. \quad (17)$$

To compare the unimorph to the bimorph, it is useful to normalize the open circuit voltage to the reference value obtained with the bimorph. The voltage can be rewritten as

$$V_p = \frac{\beta b^2}{2R}\left(\frac{h}{b}\right)\left(1-\frac{h}{b}\right) = 2\left(\frac{h}{b}\right)\left(1-\frac{h}{b}\right)V_{pb}. \quad (18)$$

The maximum value of this voltage, $(1/2)V_{pb}$, occurs when the active layer is one-half the thickness of the whole belt. Thus for the same belt thickness, this arrangement always gives a lower output voltage than the bimorph. Its advantage comes mainly in allowing us to obtain high electric fields over large diameter rollers.

We have carried out measurements of the surface potential for unimorph structures using various thicknesses for the Kynar film and for the substrate, which was a plastic shimstock. These two layers were laminated and then bent over a piece of rigid PVC tubing with a radius of 15/16 in. (23.8 mm). A comparison of the measured voltage with the values predicted using the value of β given by Eq. 11 (431 V/μm) is shown in Fig. 5. If perfect agreement was obtained, the experimental points would all lie on the diagonal line. The actual measurements bracket the line, indicating that the model is predicting the correct voltage on the average. Thus both the unimorph and the bimorph are well described by the model.

The electric field in the gap above the unimorph is given by

$$E_a = \frac{V_P}{a + h/\kappa} = \beta \frac{b}{2R} b \frac{(h/b)(1-h/b)}{(a+h/\kappa)}. \quad (19)$$

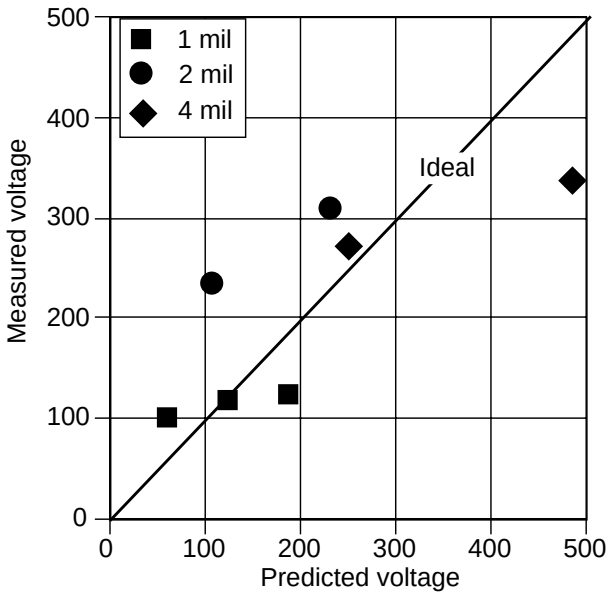

Figure 5. Unimorph voltage measurements and predictions.

Just as in the bimorph case, the largest field in the air gap occurs when the air gap is much less than the dielectric thickness of the active layer. This limiting air gap field is

$$E_{a,\lim} = \beta\kappa \frac{b}{2R}\left(1-\frac{h}{b}\right) \le \beta\kappa S_{\max}\left(1-\frac{h}{b}\right). \quad (20)$$

As an example of the effectiveness of the unimorph configuration, consider a roller with a radius of 100 mm. If the maximum strain at the surface is taken to be 1%, as before, then the thickness of the belt is obtained from

$$\frac{b}{2(100)} = 0.01 \quad (21)$$

as b = 2 mm. This is much thicker than the piezoelectric film, which is usually supplied in dimensions of a few millimeters (0.02 to 0.2 mm). If a thin piezoelectric film is mounted on top of a passive substrate, however, we can obtain performance that is even better than that of a bimorph. For example, consider a 4-mil piezoelectric film (h = 0.1 mm) mounted on a flexible substrate so that the total thickness is 2 mm, as required for maximum allowed strain. In this example,

$$\frac{h}{b} = \frac{0.1}{2} = 0.05 \quad (22)$$

and the maximum air gap field is given by

$$E_{\max} = 0.95\beta\kappa S_{\max}. \quad (23)$$

Under the same conditions, the bimorph geometry gives a maximum field that has a coefficient of 1/2, so the unimorph actually gives almost twice the output of the bimorph, while turning around a larger radius. Using the same values of piezoelectric and dielectric constants and maximum strain as used for Eq. 16, we obtain a maximum field of

$$E_{\max} = 98.3 \text{ V}/\mu\text{m}, \quad (24)$$

which is much higher than the breakdown field of air, even in very small gaps. Thus the unimorph configuration is more than adequate for obtaining fields as high as can be used in a practical machine operating in air.

Applications to Xerographic Subsystems

Although the analytical and experimental work indicates that xeromorphs are capable of generating the high electric fields needed in xerographic engines, it is always reassuring to confirm that a new device will work as well in practice as it does in the laboratory. To ensure this, we modified a commercially available Fuji Xerox laser printer to use a xeromorph field generator in the transfer step. In a separate test, the xeromorph belt was applied to charge Mylar samples. The results of these two tests are described here.

Transfer. A schematic diagram of the modified transfer subsystem is shown in Fig. 6. The bias transfer roll (BTR) has a diameter of 16.5 mm, and the photoreceptor roll (P/R) has a diameter of 60 mm. The idler roller diameter is 22 mm, and the belt moves at a process speed of 56 mm/s.

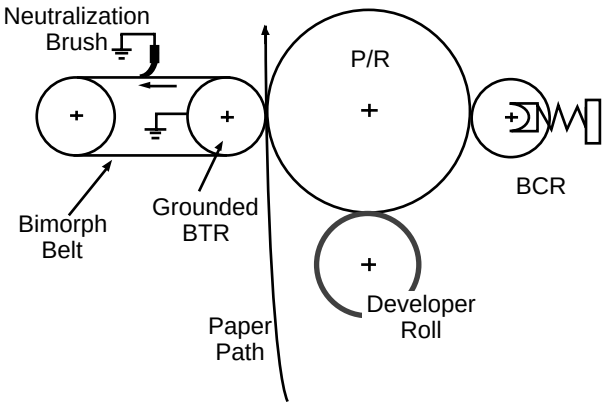

Figure 6. Application of xeromorph for xerographic transfer.

The image is transferred from the photoreceptor to the paper under the action of the electric field generated by the xeromorph riding over the grounded BTR roller. The xeromorph layer that makes up the belt is constructed as a bimorph. Along the flat portion of the belt module the xeromorph structure is in a relaxed state, which is neutralized with a conductive fiber brush. On bending around the radius of the rolls, the xeromorph structure becomes strained, resulting in a positive electric field with respect to the grounded inner conductive layer of the belt. This field attracts the negatively charged toner to the paper, completing the transfer step. Afterward, the belt passes the neutralization brush again, which serves to restore the belt surface to the uncharged state.

The neutralization brush is essential to the proper operation of a xeromorph. In this application, the belt and the paper are likely to exchange charge in the postnip region, leading to a reduction in the charge on the belt. When it straightens out, it will not return to its original uncharged state, but to a charge of the opposite polarity. If this reversed charge was allowed to remain on the belt, it would tend to cancel the electric field created during the next pass through the nip, leading to transfer failure. Similar problems arise in other applications of xeromorphs, making charge control or neutralization an important design consideration.

Figure 7 shows print samples obtained using the standard and modified engines. There is no noticeable difference between the print quality in the two cases; both used the identical process speed (56 mm/s). This result indicates that xeromorphs can replace the BTR and high-voltage power supply normally used in xerographic machines with no loss in print quality.

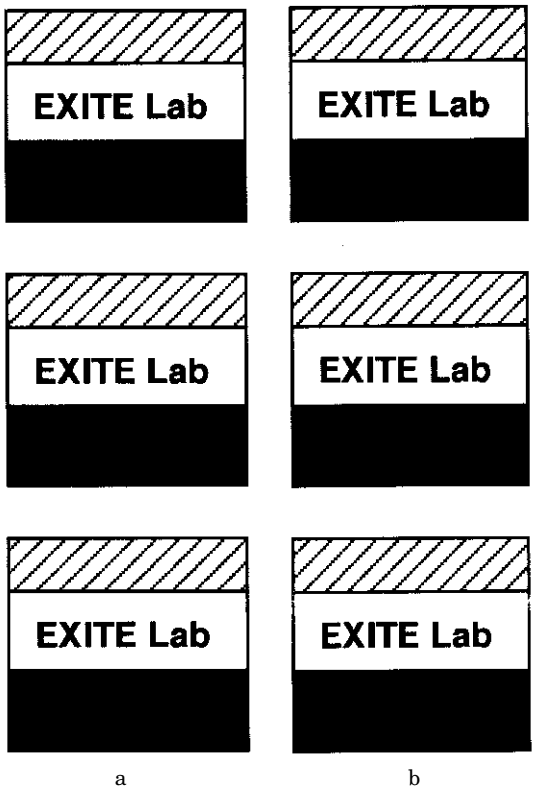

Figure 7. Xerographic prints for transfer performance comparison. (a) Conventional high-voltage power supply with BTR. (b) Xeromorph.

Receptor Charging. Another xerographic step that requires high electric fields is the charging of the photoreceptor. In the Fuji Xerox printer, this is performed by the bias charge roll (BCR) shown on the right side of Fig. 6. The BCR is maintained at a high voltage such that breakdown occurs across the air gap at the pre- and postnip regions. Unfortunately, a dc bias can sometimes lead to nonuniform photoreceptor charging as the field in the entrance nip exceeds the Paschen limit at wide spacings, resulting in cyclic breakdown events. This effect has been reported previously for charging.[4,5] This effect has also been observed when applying the xeromorph for charging in a similar manner. In a simulated photoreceptor charging experiment, a xeromorph belt was applied to charge a section of 1-mil-thick Mylar. Figure 8 shows a magnified view of the nonuniform pattern of toner that was developed, depicting the nonuniform charge pattern obtained.

In conventional BCR charging, this problem can be avoided by using ac voltages on the bias roll. To circumvent this problematic charging uniformity issue with the xeromorph, an arrangement shown in Fig. 9 was applied. The 1-mil-thick Mylar was used as a simulated photoreceptor, operating with asynchronous sliding contact. The Mylar sheet speed was always 1 ips (25.4 mm/s), and the xeromorph moved in the opposite direction at various speeds. The xeromorph itself was composed of a 110-μm-thick Kynar sheet with a 76-μm Ni back coating. The active roller had a diameter of approximately 8 mm.

Before contact with the Mylar was established, the open circuit voltage of the xeromorph at the roller was measured

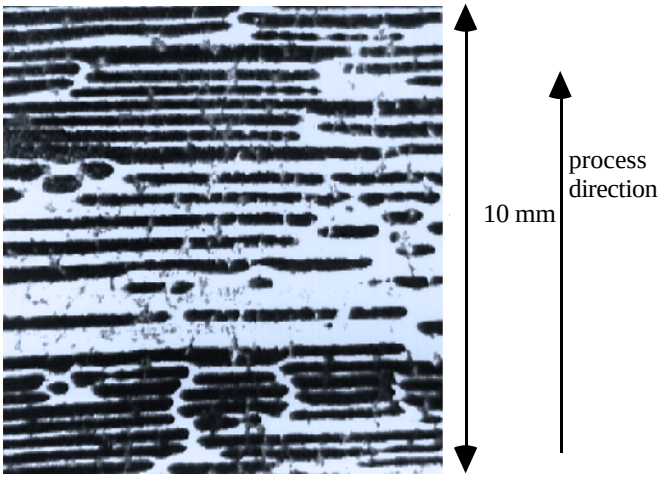

Figure 8. Nonuniform charge pattern on Mylar in process direction.

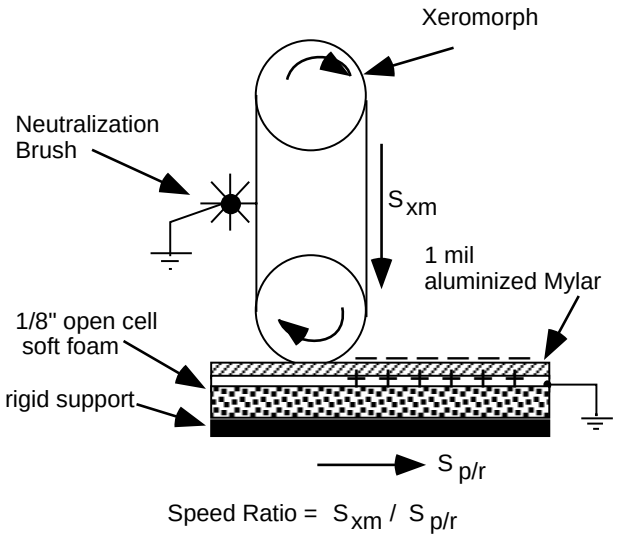

Figure 9. Xeromorph applied to Mylar receptor charging.

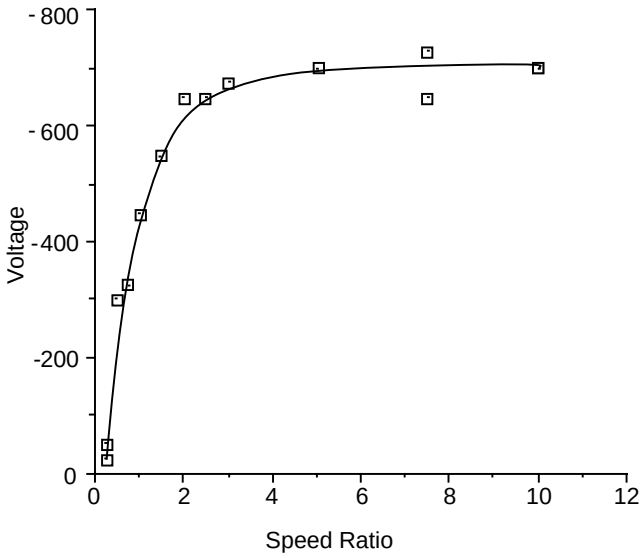

Figure 10. Surface potential versus speed ratio.

at approximately 1300 V. The voltage was on the order of voltages obtained in the work described here, but it was not possible to verify it directly against the models described because the device was neither a pure bimorph or a pure unimorph. Instead, it was composed of two materials with very dissimilar elastic properties, which would affect both the location of the neutral axis and the amount of stretching of the piezoelectric film.

Figure 10 shows a plot of the surface potential obtained as a function of the speed ratio. We speculate that above a certain speed ratio the charge stabilizes at a value just large enough to neutralize the field generated by the xeromorph. This potential is smaller than the open circuit voltage of the xeromorph, which might be expected from the additional capacitance loading due to the electroreceptor and the voltage drop needed to establish charge transport across an air gap. With this asynchronous operation, uniform charging was achieved, as indicated by visual observation of a solid area developed on the Mylar surface by standard xerographic techniques. These results suggest that the xeromorph can provide a viable alternative for photoreceptor charging, again eliminating the need for a high-voltage power supply.

Discussion

The work reported here demonstrates that piezoelectric xeromorphs can be employed to generate the high voltages and electric fields required in conventional xerography. Voltages in excess of 1 kV and fields approaching 100 V/μm have been observed in laboratory work, and xeromorphs have been used to replace conventional high-voltage power supplies in commercially available xerographic engines.

Whereas the current output is apparently sufficient for the low-speed applications described here, the question of higher speeds is always of practical interest, because higher speeds draw more current, and therefore more power, from the device. At any speed, the charge is generated by the bending of the piezoelectric material. The work done by the charge in transferring toner (or charging the surface of a photoreceptor) therefore comes from the mechanical work done in bending the piezoelectric film, which operates over a closed electromechanical energy conversion cycle. The amount of charge generated per cycle is controlled by the amount of deformation and not by its rate. When the belt moves at a higher speed, it supplies the same charge per cycle, but the cycles repeat faster, thus giving a higher output current. This behavior means that the device is basically insensitive to speed when used in a typical xerographic application. Of course, resistive or mechanical losses could reduce the output at very high speeds, but these effects cannot be addressed in the lossless model presented here.

Acknowledgments. The authors wish to acknowledge the inputs provided by Peter D. McAnn, Andrew B. Radcliffe, and Michael S. Smith.

References

1. T. T. Wang, J. M Herbert, and A. M. Glass, Eds., *The Applications of Ferroelectric Polymers*, Blackie and Son Ltd., Glasgow (1988).
2. J. M. Crowley, *Fundamentals of Applied Electrostatics*, Krieger (1991).
3. R. Holland and E. P. EerNisse, *Design of Resonant Piezoelectric Devices*, MIT Press, Cambridge, Massachusetts, pp. 3ff.
4. H. Kawamoto and H. Satoh, Numerical simulation of the charging process using a contact charger roller, *IS&T's 9th International Congress on Advances in Non-Impact Printing Technologies/Japan Hard Copy '93,* Yokohama, Oct. 1–5, 1993, pp. 2, 81.
5. K. W. Pietrowski and Dennis W. Vance, Studies of an air discharge between a metal roller and a insulating plane with applications to TESI and roller charging, Xerox Internal Report **69-14** (1969), to be published.